Groundwater Research Report
WRC GRR 95-09

NEAR SOURCE TRANSPORT OF CONTAMINANTS IN HETEROGENEOUS MEDIA

John A. Hoopes
Salwa M. Rashad
Tswn-Syau Tsay

1995

NEAR SOURCE TRANSPORT OF CONTAMINANTS IN HETEROGENEOUS MEDIA

John A. Hoopes
Salwa M. Rashad
Tswn-Syau Tsay
Department of Civil and Environmental Engineering
University of Wisconsin-Madison

Groundwater Research Report
WRC GRR 95-09
University of Wisconsin System
Groundwater Research Program

Water Resources Center
University of Wisconsin-madison
1975 Willow Drive
Madison, Wisconsin

1995

This project was supported, in part, by General Purpose Revenue funds of the State of Wisconsin, to the University of Wisconsin System for the performance of research on groundwater quality and quantity. Selection of projects was conducted on a competitive basis through a joint solicitation from the University and the Wisconsin Departments of Natural Resources; Agriculture, Trade and Consumer Protection; Industry, Labor and Human Relations; and with the concurrence of the Wisconsin Groundwater Coordinating Council.

ABSTRACT

Waste spills, landfill and storage facility leaks, and recharged surface waters introduce substances over small areas to groundwater. Resulting substance distributions generally exhibit spatial and temporal variability due to geologic and source property variations. Knowledge of the transport and fate of contaminants in the subsurface environment is vital to successful groundwater quality management efforts that aim to protect "clean" groundwater and clean up "contaminated" groundwater. Defining the flow pattern (velocity magnitude and temporal and spatial variations) is key to determining contaminant concentration distributions and rates of movement.

Two problems were investigated: (1) movement and mixing of a miscible, buoyant liquid plume in flowing groundwater; and (2) mounding, flow pattern, and contaminant distribution of water recharge to a water table aquifer.

The objectives were to: (1) understand and characterize effects of media heterogeneity, transient flow, loading conditions and substance density on the movement and mixing of contaminants for these cases; (2) develop predictive models for these phenomena with steady and transient conditions; and (3) conduct laboratory experiments to determine model parameters and test models.

Regulatory agencies and operators of land disposal facilities who must place and sample monitoring wells for the detection of contaminants will find the results of this project valuable. In addition, consulting firms involved with spill clean up and determining the impacted area and spreading from the area will benefit from this project's findings. Agencies and firms who design and license groundwater recharge facilities and must determine the mounding, penetration, and spreading of the recharged water will also find this research helpful.

CONTENTS

FIGURES

NOTATION

E	Seepage potential (L^3/T)
h_0	See Figure 2
h_s	See Figure 2
h_w	See Figure 2
H(x)	See Figure 2
K	Hydraulic conductivity (L/T)
L	See Figure 2
N	Recharge rate (L/T)
p	Pressure (F/L^2)
z	Elevation head (L)
γ	Specific weight of water (F/L^3
ϕ	Piezometric head (L)
x,y,z	Orthogonal, cartesion coordinates
ζ,μ,η	Orthogonal, ellipsoidal coordinates
Δt	Time step
Δx	Cell length
t	Time
a	Half of distance between major foci of ellipsoidal heterogeneity
C_c	Cell Courant number ($V_{max}\,\Delta t/\Delta x$)
P_{eg}	Grid Peclet number ($V_{max}\,\Delta x/D$)

MOVEMENT AND MIXING OF A MISCIBLE, BUOYANT LIQUID PLUME IN FLOWING GROUNDWATER

INTRODUCTION

A three-dimensional, particle tracking scheme is used to compute the trajectory of and spread about the centroid of a mass slug added to steady flow through an infinite aquifer with an ellipsoidal heterogeneity (hydraulic conductivity different from the aquifer). Particles are moved and mixed using local velocity and dispersion values. The effects of hydraulic conductivity, size and position of the heterogeneity and of source density on the plume trajectory and spread are investigated and compared with a plume in a homogeneous aquifer.

Buoyant, contaminant groundwater plumes occur when wastes, having densities different from groundwater, are released into the subsurface, saturated environment. Resulting contaminant distributions exhibit spatial and temporal variability due to geologic, source, and waste variations. Defining the flow pattern (velocity magnitude, temporal and spatial variations) is necessary to determine contaminant concentration distributions and rates of movement. This study seeks to identify and quantify the effects of media heterogeneity on plume movement and mixing, and conduct laboratory experiments to test the predictive model and evaluate their parameters.

REVIEW OF AVAILABLE METHODS

To predict solute transport by contaminant plumes the ambient flow field must be known. Introducing a plume alters this ambient flow field due to density-induced motion. The concentration distribution and plume trajectory are determined from the ambient velocity field and the plume dynamic equations. There are two basic approaches to investigate the plume behavior: (1) solve the flow field and the solute transport equations simultaneously; or (2) develop the ambient flow field and use it in the transport model. The second approach is more efficient; however, it is restricted to dilute concentrations (i.e., pollutant does not affect the flow field).

There are various approaches to determine the ambient flow field in heterogeneous media. A deterministic approach would apply if large-scale heterogeneity (i.e., features such as layers or lenses) can be located and its material and hydraulic properties determined. If it is difficult to fully characterize the heterogeneous media, stochastic or probabilistic approaches (Dagan, 1989) are more appropriate.

Most analytical solutions are restricted to relatively simple geometries and boundary conditions. This limitation can sometimes be overcome by superimposing many analytic solutions allowing the total solution to meet irregular boundary conditions (e.g., Strack, 1989). Analytic solutions give insight into the dependence of the solution on various physical parameters, such as hydraulic conductivity or geometrical dimensions.

Numerical methods consist of certain procedures which replace the governing partial differential equations by a system of algebraic equations, which are then solved. The various numerical methods

differ mainly in the way the system of equations are derived. The most popular and powerful methods for numerical solution are the analytic element method, the boundary integral element method, and the finite difference and finite element methods. Each of these methods was reviewed to determine its advantages and limitations for computing plume characteristics. Based on the extensive calculations in any of these numerical schemes and in order to take advantage of analytic solutions, a combined analytic/numeric method is adopted.

The development and implementation of a model to simulate the movement and mixing of miscible, buoyant, contaminant plumes in saturated porous media with a single heterogeneity is presented here. Representation of multiple heterogeneities will be based upon this model.

THEORETICAL MODEL

Flow Field

For steady flow through a rigid, saturated porous media the piezometric head, ϕ, is governed by

$$\nabla^2\phi = 0 \tag{1}$$

where $\phi = p/\gamma + z$. Aquifer heterogeneity is modeled as a single, homogeneous, isotropic, oblate ellipsoid of hydraulic conductivity K_1, and is located in an infinite, isotropic, homogeneous media of hydraulic conductivity K_2 (Figure 1). An oblate ellipsoid is obtained by revolving an ellipse about its short axis. The ellipsoid shape varies with its eccentricity value, so it enables the simulation of almost any shape of heterogeneity. The equation of an oblate ellipsoid with coordinates centered at its origin is

$$\frac{x^2 + y^2}{1 + \zeta_o^2} + \frac{z^2}{\zeta_o^2} = 1 \tag{2}$$

The Cartesian coordinates (x,y,z) are normalized by "a", the half-distance between the major foci of the spheroid, and are related to ellipsoidal coordinates (ζ,μ,η) by

$$x = \sqrt{(1-\mu^2)(1-\zeta^2)}\cos\eta;\ y = \sqrt{(1-\mu^2)(1+\xi^2)}\sin\eta; \tag{3}$$

$$z = \mu\zeta;\ 0<\zeta<\infty;\ -1<\mu<1;\ 0<\eta<1$$

The solution to Eq. (1) for uniform flow within and far from the heterogeneity is given by

$$\phi_1 = Bx \tag{4}$$

$$\phi_2 = -Jx + A\left\{\frac{\zeta}{1+\zeta^2} - \cot^{-1}\zeta\right\}x.$$

ϕ_1 and ϕ_2 are the piezometric heads within and outside the heterogeneity, respectively, normalized by "a." A and B are constants, determined by equating the head and normal flux on both sides of the heterogeneity. $J = q_\infty/K_2$, where q_∞ is the uniform velocity far upstream from the heterogeneity.

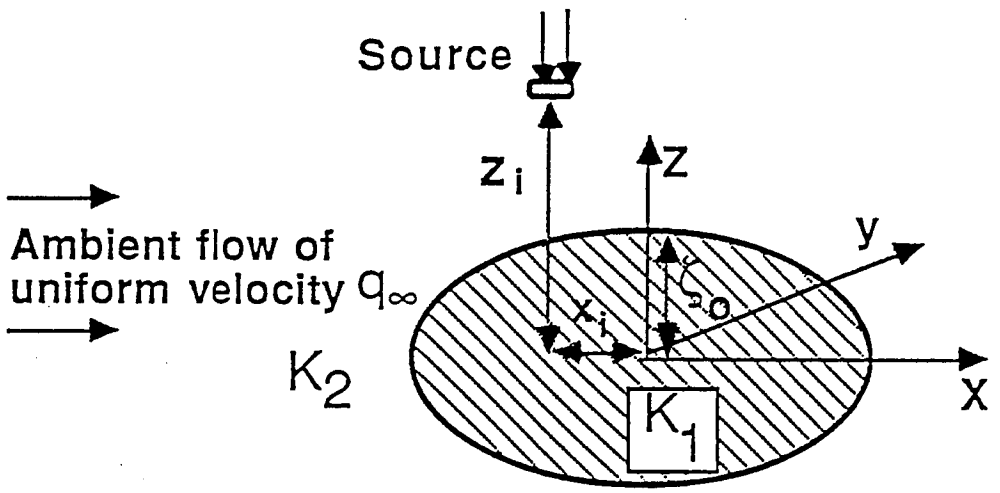

Figure 1. Flow field, heterogeneity and coordinates.

Contaminant Distribution

The distribution of a dissolved, conservative species is governed by the mass balance equation

$$\frac{\partial(\theta C)}{\partial t} + \frac{\partial(\theta C V_i)}{\partial X_i} - \frac{\partial}{\partial X_i}\left(\theta D_{ij}\frac{\partial C}{\partial X_j}\right) = 0 \tag{5}$$

where C = concentration, θ = porosity, V_i = i^{th} component of interstitial velocity, and D_{ij} = local hydrodynamic dispersion tensor, which can be written

$$D_{ij} = (\alpha_T V + D_o)I_{ij} + (\alpha_L - \alpha_T)\frac{V_i V_j}{V} \tag{6}$$

where V is the magnitude of the velocity, α_L and α_T are local longitudinal and transverse dispersivities, respectively, I_{ij} is the identity tensor, and D_o is the molecular diffusivity in porous media.

Choice of Numerical Approach for Transport Simulation

Due to the complexity of both the flow and transport problems an uncoupled approach is used in which the flow field is developed independently of the plume. This velocity field and the density-induced velocity are input to the transport code.

There are a number of numerical approaches for solving the transport problem (e.g., finite element, finite difference, or random walk particle methods). Conventional finite element or finite difference approaches will require the solution of N_g algebraic equations, where N_g is the number of grid points, and a computational expense proportional to $N_g^{+\eta}$, where η, which depends on the method, lies in the range $0<\eta\leq 1$. In the random walk particle method (RWPM), the computational effort per time step for a conservative, one-component substance is proportional to the number of particles (N_p) used. With as many as 10^6 nodes being considered and with 100 particles being sufficient for a one-component model (Ahlstrom et al., 1977), it is clear that the particle approach is the efficient choice for computational efficiency.

As a first approximation dispersion and dilution effects were neglected. A computer model was developed using "Mathematica" software on a Macintosh PCII to calculate head and velocity components at any point in space and plume trajectory for specified values of heterogeneity hydraulic conductivity, size, shape and porosity, of source density, and of aquifer hydraulic conductivity and flow gradient.

Particle Tracking Using Random Walk Approach

In RWPM the solute mass is presented as a large collection of particles which are small, identical, unchanging amounts of mass. These particles are individually moved through space by advective and dispersive processes over a discrete time step.

The trajectory of and spreading about the centroid of a conservative, buoyant, miscible slug of mass introduced at source (Figure 1), are computed by a modified form of Tompson et al.'s (1987, 1990) particle tracking scheme. The interaction between desnity and heterogeneity on the ambient flow field is ignored in this work. Each particle is moved in a sequence of steps, each step involving advection and dispersion using (local) conditions at each point. Thus, the particle position x, at any time, $t + \Delta t$, is given by

$$x_i(t+\Delta t) = x_i(t) + A_i(t)\Delta t + B_{ij}R_i\sqrt{\Delta t}, \qquad (7)$$

where

$$A_i = V_i + \frac{\partial D_{ij}}{\partial x_j} + \frac{D_{ij}}{\theta}\frac{\partial \theta}{\partial x_j}, \quad B_{ij}B_{jk} = 2\,D_{ik}\,,$$

and R_j = set of 3 random numbers (zero mean and variance of one). The centroid, $\bar{x}_i$ (t), and the variance, $\sigma_{ii}(t)$, of the N_p particles are given by

$$\overline{x_i} = \frac{1}{N_p} \sum_{i=1}^{N_p} x_i(t)$$

and (8)

$$\sigma_{ii}^2 = \frac{1}{N_p} \sum_{i=1}^{N_p} (x_i(t) - \overline{x_i})^2 .$$

As the number of particles becomes large, the results approximate a continuous slug of mass and the governing equation for the particle distribution [Fokker-Planck] becomes that for a continuous concentration distribution.

Particles are introduced at the source with a vertical buoyant velocity=w=-K$\Delta\rho/\rho$, where K = hydraulic conductivity of the medium and $\Delta\rho/\rho$ = dimensionless density difference between the source and ambient. The particle buoyant velocity is added to the vertical ambient velocity.

Introducing Dilution Effects

The density difference between the plume and the ambient flow is continuously decreased due to dilution effects along the plume trajectory. To account for dilution the local (in each cell) density is computed after each time step as

$$\Delta\rho(x_i, t) = \frac{m\ N_{p\ i}(x_i, t)}{vol\ \theta(x_i)} \quad (9)$$

where m = mass allocated to each particle, N_{pi} = number of particles in the cell surrounding x_i at time t, vol = cell volume, and θ = cell porosity. The density-induced velocity, w (x_i, t), is calculated from

$$w(x_i, t) = -K(x_i) \frac{\Delta\rho(x_i, t)}{\rho} \quad (10)$$

In this manner the vertical buoyant velocity of the plume is reduced as the plume spreads.

Application of the Model

The transport model [Eqs. (7-10)] and the flow model [Eqs. (1-4)] are applied to different types of boundary and initial conditions. The first case is an initial slug of mass M at position x_o. The second case is a source of constant discharge Q of contaminant with concentration C_o at position x_o. For both cases the boundary and initial conditions must be represented by appropriate particle distributions.

For the initial slug case the total mass M is represented by a number of particles N_p randomly distributed in the cell surrounding the location x_o at time t = 0. The particles then are advected and dispersed according to Eq. 7. For the continuous source case, a constant number of particles, N_{pf}, per unit time per unit area are introduced into the boundary with centroid at x_o. The mass allocated to each particle is computed as $m = QC_o/(N_{pf}\, dA)$, where dA is the area normal to the contaminant flux.

SAND TANK EXPERIMENTS

The design of an experimental apparatus and planned tests are described. A laboratory sand tank will be used to test the model of plume characteristics in a heterogeneous, confined aquifer having a small sphere of hydraulic conductivity K_1 surrounded by porous media of K_2. The sphere and porous media are isotropic and homogeneous. Plume characteristics of interest include spreading, trajectory, and concentration distribution. The aquifer will be fully saturated and have a steady, uniform flow through it. The source introduction area will be small so that point source conditions are expected to govern plume characteristics.

The experimental setup and laboratory procedure were based on the work of Paschke and Hoopes (1984). The apparatus is a closed, rectangular sand tank; one side of the tank is glass, while the remaining sides, top, and bottom are aluminum. The spherical heterogeneity (3-cm radius was made of fine, nearly uniform sand, bonded by water resistant epoxy) is surrounded by a coarse, nearly uniform sand. The ratio of hydraulic conductivity between the coarse and the fine sand is about 10 to 1. Piezometer ports, four along the top and four along the bottom of the tank, are used to determine the flow uniformity, gradient, and the hydraulic conductivity of the surrounding coarse sand. An electronic pressure transducer is used to obtain pressures at various points near the heterogeneity surface.

A solution of salt water ($NaNO_3$) representing the contaminant plume source, will be introduced through a small opening (0.79 cm diameter) in the sand tank cover. $NaNO_3$ was selected as the contaminant solute because it is very soluble in water and is not as corrosive as NaCl. Forty-nine sampling ports (7 columns of sampling ports with 7 ports in each column) are provided for extracting fluid samples from the sand tank; the ports in rows 1, 2, 3, 5, and 7 contain one sampling tube which penetrates to the tank centerline while the ports in rows 4 and 6 contain five tubes each, evenly spaced across the tank width at 5 cm increments. The sampling tubes are hollow brass tubes 30 cm long with an inside diameter of 0.84 mm. The salt concentration of the samples will be determined using a conductivity meter.

Coarse sand will be densely packed in a dry condition until the appropriate level for heterogeneity insertion is reached. The sphere will be placed in the tank and packing of the coarse sand was continued to the top as previously described. A layer of sponge rubber will be placed over the top of the sand and the tank cover bolted in place. To ensure a saturated conditions the tank will be slowly filled with degassed water from the bottom.

To begin a test, room temperature water is circulated through the tank at the desired rate and a known concentration and rate of $NaNO_3$ solution is introduced at the source.

Piezometric heads are observed on the manometer bank to determine the flow uniformity, gradient, and hydraulic conductivity through the coarse sand. Pressure differentials are monitored by the electronic pressure transducer to obtain the head distribution in the region of the heterogeneity.

The experiment will be left undisturbed until the plume reaches steady conditions. Samples of 4 ml will be taken from each sampling tube proceeding from the downstream ports to the upstream ones; the samples will be collected in test tubes and transferred to the conductivity cell using an eye dropper. The sample volume of 4 ml provides enough fluid to rinse and fill the conductivity cell and recheck the reading, and yields a "spatially averaged" concentration over a sphere of radius 1.36 cm in the medium. Upon completion of the sampling,t he freshwater (ambient) flow rate, piezometric heads and pressure differentials will be checked.

Separate experiments have been conducted in the sand tank for determining longitudinal and lateral dispersion coefficients.

RESULTS AND DISCUSSION

Computer results were compared with analytical solutions for homogeneous, uniform flow cases. The agreement and the smoothness of the results are dependent on the number of particles N_p, cell courant number, $C_c = V_{max}\Delta t/\Delta x$, and grid Peclet number $P_{eg} = V_{max}\Delta x/D$, where V_{max} denotes the maximum speed in the flow field, and D denotes a typical element of the dispersion tensor. The errors in the first and second moments of the particle distributions were less than 1% for $2<P_{eg}<4$, and $C_c<0.2$. Results with Mathematica for no dispersion compared well with the RWPM results for zero dispersivity.

After performing these checks on the computer model, it was used to investigate the heterogeneity and source buoyancy effects on plume behavior. The trajectory and spreading of the plume were computed at a nondimensional time $K_2\, t/a = 100$, for all cases. The smoothness of the trajectory and spreading are affected by the number of particles (results, herein, are based on 50 particles). The time step, $\Delta t = 0.2\ \Delta x/V_{max}$, was chosen to minimize errors in the displacement computation (7).

Figures 2 and 3 demonstrate the effect of hydraulic conductivity ratio, $\epsilon = K_1/K_2 = 0.1$, 1.0 (homogeneous) and 10.0 on the trajectory of and spreading about the centroid of a slug of mass. x_{CL} and z_{CL} define the mass centroid with respect to the heterogeneity, and spreading is represented by σ_{pp} which is proportional to the slug volume. The presence of the heterogeneity causes the trajectory to penetrate deeper into the medium than for the homogeneous case. For $\epsilon < 1$ the penetration depth is less and the plume trajectory is shorter than the homogeneous case. The heterogeneity increased spreading compared to a homogeneous media. For $\epsilon < 1$ spreading is markedly increased due to deflection of the flow around the heterogeneity compared to $\epsilon > 1$ where flow passes through to the heterogeneity.

Calculations were made to determine the effect of heterogeneity position (relative to the source) and size ($4\pi\zeta_o[1 + \zeta_o]$) and of source buoyancy ($\Delta\rho/\rho$) on the trajectory of and spreading about the

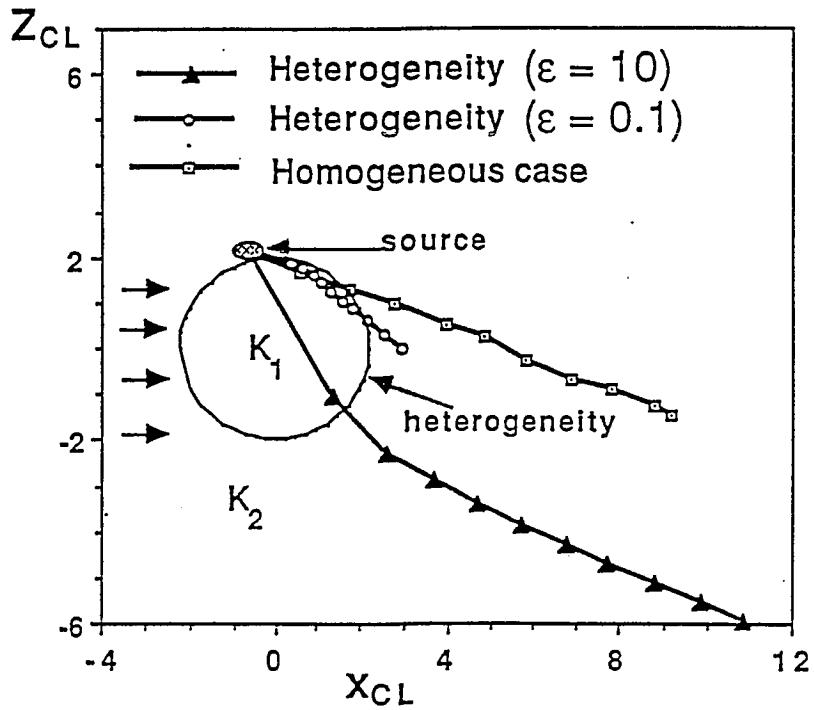

Figure 2. Effects of conductivity contrast on plume trajectory for initial slug case using constant buoyant plume density along the trajectory ($\zeta_o = 2.0$, $\Delta\rho/\rho = 0.04$, x_i, y_i, z_i, = -0.75, -0.25, 2.0).

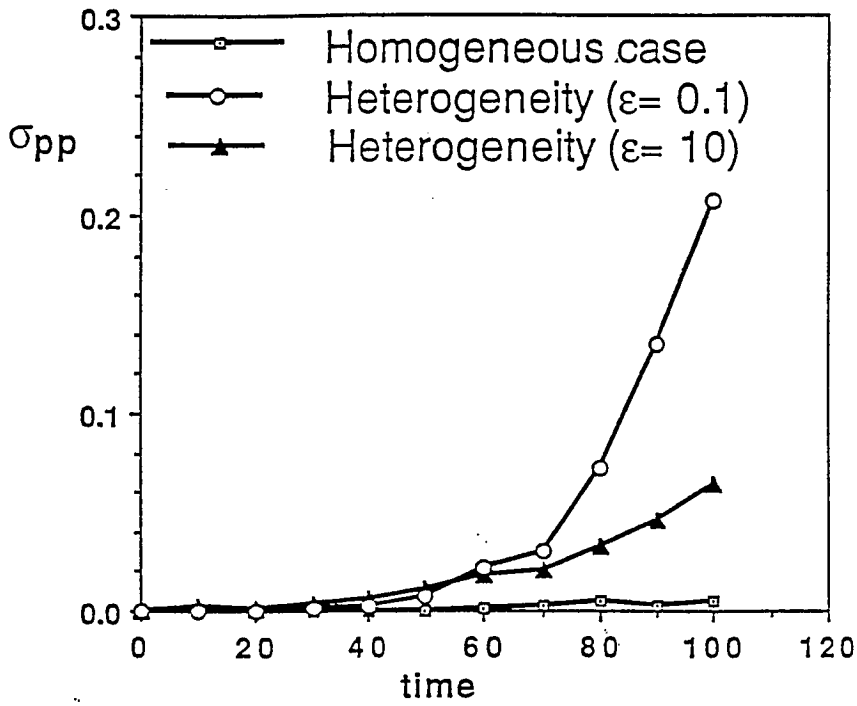

Figure 3. Effects of conductivity contrast on plume spreading for initial slug case using constant buoyant plume density along the trajectory ($\zeta_o = 2.0$, $\rho/\rho = 0.04$, x_i, y_i, z_i, = -0.75, -0.25, 2.0).

centroid of a mass slug. Moving the heterogeneity farther from the source (other factors held constant) reduces its effects on the trajectory and spreading of the mass slug. For $\epsilon < 1$ as the heterogeneity size increased, the vertical penetration decreased and the spreading of the mass slug increased. Further, with $\epsilon < 1$ as $\Delta\rho/\rho$ decreased, the spreading of the mass slug decreased, while the vertical penetration increased.

After modifying the transport model to include dilution, the plume trajectory and spreading were computed for various conditions (Figures 4 and 5). Comparing Figures 2 and 4 shows that neglecting dilution overemphasized buoyancy effects on the trajectory causing the plume to move down through the heterogeneity ($\epsilon = 10$ and $\Delta\rho/\rho = 0.04$). Comparing Figures 3 and 5 shows that neglecting dilution causes more rapid spreading ($\epsilon = 10$ and $\Delta\rho/\rho = 0.04$). Finally, for the homogeneous case buoyancy has a small influence on trajectory and spreading; however, neglecting buoyancy for the heterogeneous case results in significant effects on plume trajectory (Figures 4 and 5).

The computations of the continuous source cases are sensitive to P_{eg}. P_{eg} values > 2-4 severely affected the solution near the source where sharp gradients of concentration exist.

CONCLUSIONS

An analytic/numeric model has been developed for computing the trajectory and spread of slug or continuous injections of a miscible, buoyant substance into flowing groundwater through an aquifer with an ellipsoidal heterogeneity. The model has been verified for simple known cases. The model was used to show the effects of heterogeneity size, position and hydraulic conductivity and of source density on plume behavior.

Numerical results demonstrate that it is essential to include the interaction between buoyancy and heterogeneity in predictive models for plume trajectory and spreading. Furthermore, it is necessary to account for dilution in calculating buoyancy effects. Decreasing the size of the heterogeneity or moving it farther from the source reduces its effects.

Experimental tests in a sand tank (confined) with a single, ellipsoidal heterogeneity are being initiated to measure the trajectory and concentration distribution of a salt water plume discharged into uniform flow through the tank and to compare with the model predictions. Consideration is being given to altering the model to include interaction between heterogeneity and buoyancy on the ambient flow. Finally, this work is envisioned as a first step to modeling flow and plume behavior in realistic models of aquifers. Subsequent work will seek to represent aquifer heterogeneity by randomly choosing the size, orientation, hydraulic conductivity and position of such ellipsoidal regions in an aquifer and introducing a buoyant plume; incorporation of solute-media reactivity is also planned.

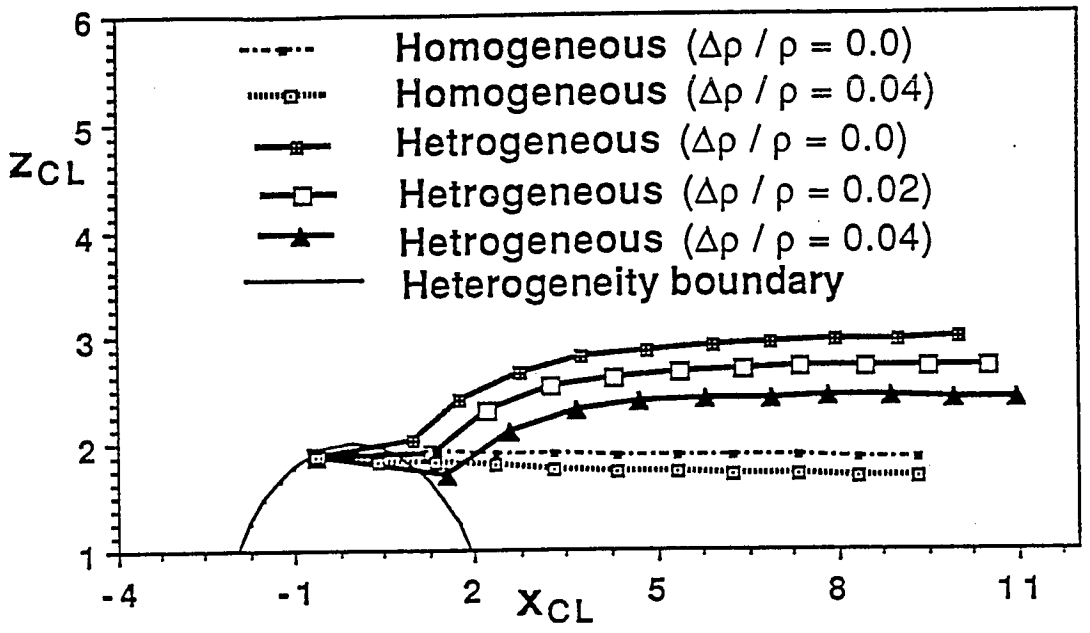

Figure 4. Effects of source buoyancy $\Delta\rho/\rho$ on plume trajectory for initial slug case using variable buoyant plume density along the trajectory for ($\zeta_o = 2.0$, $\epsilon = 10$, x_i, y_i, z_i, = 0.75, -0.25, 2.0).

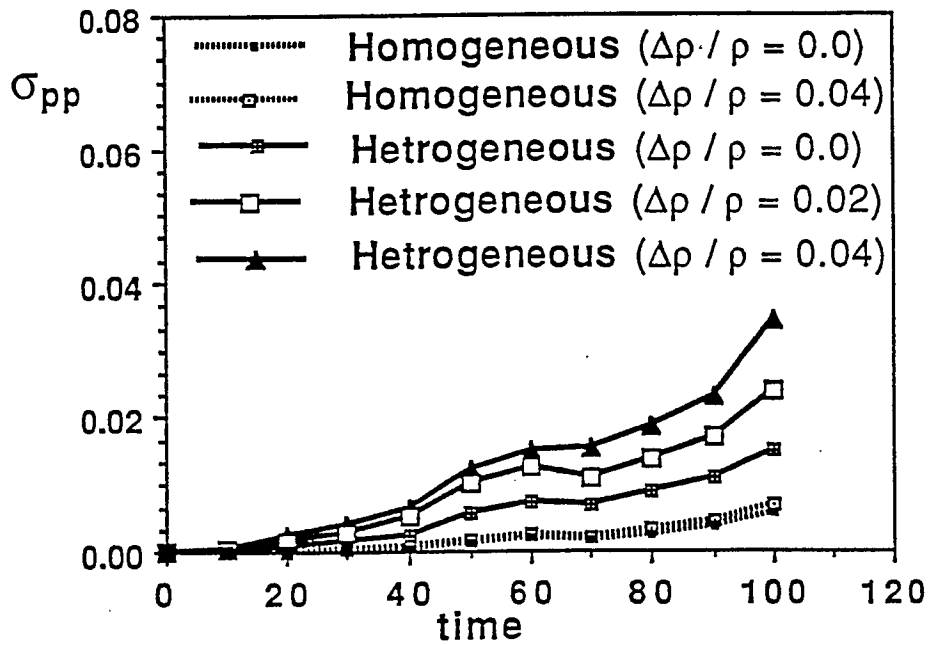

Figure 5. Effects of source buoyancy $\Delta\rho/\rho$ on plume spreading for initial slug case using variable buoyant plume density along the trajectory for ($\zeta_o = 2.0$, $\epsilon = 10$, x_i, y_i, z_i, = 0.75, -0.25, 2.0).

MOUNDING, FLOW PATTERN AND CONTAMINANT DISTRIBUTION OF WATER RECHARGE TO A WATER TABLE AQUIFER

INTRODUCTION

Groundwater mounding due to local recharge is generally computed from a solution of the Forchheimer equation using the Dupuit assumptions. These assumptions are closely approximated when the water slope is small -- usually <0.01. In this work a general analytic/numeric method for solving the governing (Laplace) equation is developed which incorporates vertical motion and the seepage face and does not require a small water table slope. The unknown coefficients and height of the water table in the series solution are obtained by solving a system of nonlinear equations which satisfy the seepage potential and potential function conditions on the phreatic surface. Use of the seepage potential condition on the water table may enable a direct extension of this work to heterogeneous aquifers. The results of this new method indicate a good estimation of the phreatic surface (water table) except the seepage face height; alternate ways to formulate this condition are under investigated.

Groundwater mounding is caused by local recharge (usually from a land fill or a waste site) to the saturated zone in an unconfined aquifer. The shape and height of the mound depend on many factors including the geometry of the local recharge, the rate of supply of leachate, the geologic structure and the chemical and physical characteristics (e.g., hydraulic conductivity and its variations) of the aquifer, the location of controls (e.g., drains, wells, streams, marshes), the saturated thickness of the aquifer and the natural (regional) groundwater flow pattern. Figure 6 is an example of groundwater mounding.

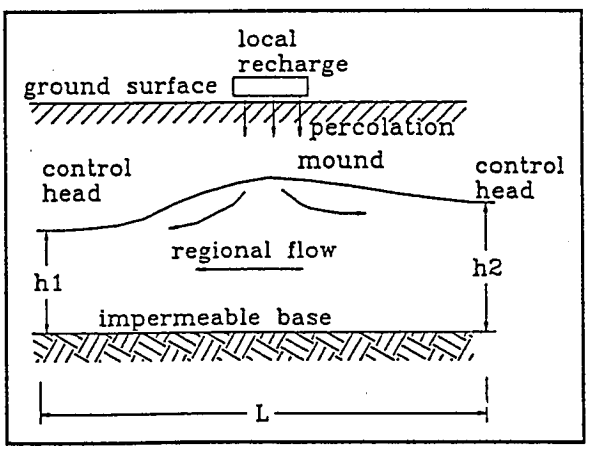

Figure 6. Example of groundwater mounding.

Groundwater mounding of the water table occurs until sufficient gradients (slopes) develop to transport the local recharge away. The resulting flow pattern depends on aquifer and recharge characteristics. These phenomena are governed by Darcy's equation and the law of mass

conservation (continuity equation). The governing equation is Laplace's equation with appropriate initial and boundary conditions. The conditions on the phreatic surface (water table) are nonlinear. Various techniques have been applied to circumvent this difficulty such as the application of the Dupuit assumptions and linearization (Strack, 1984; Voorhess, 1989; Hantush, 1967). Solutions, based on these simplifications, are not valid in regions of steep hydraulic gradients (>0.01) because vertical flow and horizontal flow must be considered.

Objectives of this portion of the study include: (1) reviewing and evaluating existing models and methods for computing groundwater mounding; (2) developing a model to predict mounding, flow pattern and contaminant distribution in heterogeneous aquifers; and (3) conducting laboratory experiments to test this model and to determine model parameters.

Youngs (1965) applied Girinskii's (1946) discharge potential to obtain an estimate of the range in steady water table heights in soils with hydraulic conductivity varying with depth for fixed boundary conditions. The seepage potential can be used to determine the flow pattern in heterogeneous aquifers.

Kirkham and Powers (1964) obtained an exact theoretical solution to Laplace's equation for a case with constant heads on the boundaries, including a seepage face. The method requires finding the coefficients in the series solution and the phreatic surface water table height by matching the water table stream function and the potential function at a number of locations between real and imaginary domains (below and above the water table, respectively). Murray (1970) solved the same problem as Kirkham and Powers (1964) using a spline function. A trial and error method was used to find the right position of the water table. He also showed that the Kirkham and Powers (1964) method does not converge to the correct seepage height.

Brock (1976) compared solutions to the Forchheimer equation (analytical), linearized potential solution of Laplace's equation and the exact solution of Laplace's equation (numerical) for local recharge in a homogeneous aquifer. His results showed the effects of aquifer and recharge conditions on accuracy in estimating water table mounding.

MOD flow is a finite-difference model used to simulate three-dimensional groundwater flow in unconfined and confined aquifers. It also can simulate groundwater flow for heterogeneous and homogeneous media. This numerical model computes flow patterns in unconfined aquifers but neglects the seepage face.

Voorhees (1989) conducted laboratory experiments on groundwater mounding in homogeneous and heterogenous (uniform layers of different sizes of sand), water table aquifers for stationary and flowing ambient conditions. His experiments showed that heterogeneity significantly affected the water table height and flow pattern.

MATERIALS AND METHODS

Methods to incorporate vertical motions and the seepage face in solutions to Laplace's equation were investigated. These solutions are written in series form with coefficients determined by matching boundary conditions on the water table whose position is found as part of the solution. A numerical solution is required of these simultaneous, nonlinear equations. The approach is first applied to a simple case to test its validity.

Mathematical Statement for a Simplified Case

Figure 7 is a sketch of the flow field and boundary conditions for steady flow through a homogeneous earth embankment. It is assumed that: (1) the aquifer is homogeneous and isotropic; (2) the aquifer lies on a horizontal impermeable stratum; (3) the aquifer is saturated below the water table; (4) capillary effects are negligible and water is released instantaneously from storage with a decline in pressure; (5) no recharge or evaporation occurs to or from the water table; (6) the aquifer skeleton is rigid, and water is incompressible; (7) Darcy's law is valid; (8) the lateral extent of the aquifer is finite; and (9) the aquifer is bounded by two vertical faces (distance L apart) with constant head on one side and a seepage face and constant head on the other side.

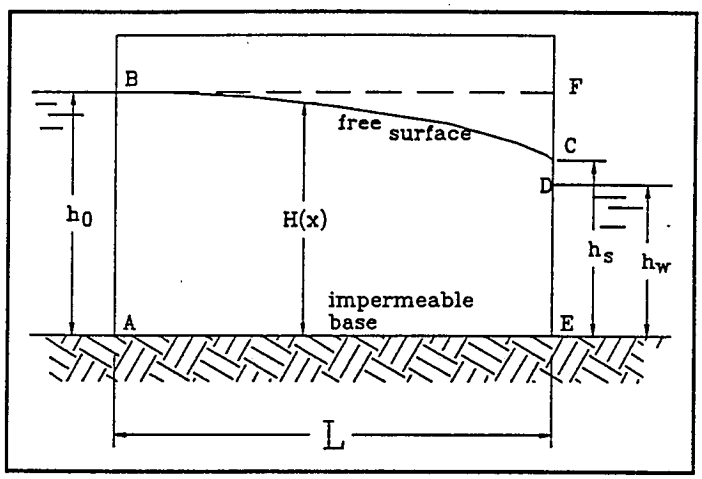

Figure 7. Configuration of the simplified case.

The governing Laplace equation is

$$\nabla^2\phi = 0 \quad where\ \phi = \frac{p}{\gamma} + z \tag{11}$$

The boundary conditions are

$$\frac{\partial\phi}{\partial z} - \left(\frac{\partial\phi}{\partial x}\right)^2 - \left(\frac{\partial\phi}{\partial z}\right)^2 = 0 \quad on\ z = H(x) \tag{12}$$

$$\phi = z \quad on\ z = H(x) \tag{13}$$

$$\phi = h_0 \quad on\ x = 0 \tag{14}$$

$$\frac{\partial \phi}{\partial z} = 0 \quad on\ z = 0 \tag{15}$$

$$\phi = h_w \quad on\ x = L\ for\ 0 \le z \le h_w \tag{16}$$

$$\phi = z \quad on\ x = L\ for\ h_w \le z \le h_s \tag{17}$$

The general solution of Eq. (11) can be expressed as:

$$1 + A_0 \frac{x}{2L} + \sum_{p=1}^{\infty} A_p \frac{\sinh(\frac{p\pi x}{h_0})}{\sinh(\frac{p\pi L}{h_0})} \cos(\frac{p\pi z}{h_0}) + \sum_{m=1}^{\infty} B_m \frac{\cosh(\frac{m\pi z}{L})}{\cosh(\frac{m\pi h_0}{L})} \sin \tag{18}$$

At x = L, Eq. (18) reduces to be

$$\phi = h_0 \left(1 + \frac{A_0}{2} + \sum_{p=1}^{\infty} A_p \cos(\frac{p\pi z}{h_0}) \right) \tag{19}$$

Applying Eqs. (16) and (17), A_0 and A_p can be calculated from Fourier theory as

$$A_0 = \frac{2}{h_0} \left[\frac{h_w^2}{2h_0} + \frac{h_s^2}{2h_0} - h_s \right] \tag{20}$$

$$\frac{2}{p\pi} \sin\left(\frac{p\pi h_w}{h_0} \right) + \frac{2}{p\pi h_0} \left[h_s \sin\left(\frac{p\pi h_s}{h_0} \right) + \frac{h_0}{p\pi} \cos\left(\frac{p\pi h_s}{h_0} \right) \cos \right| \tag{21}$$

The solution, Eq. (18) satisfies boundary conditions (14 to 17). The unknown coefficients, B_m, and water table height, H(x), are obtained by satisfying Eqs. (12) and (13) at a number of "x" locations.

To extend the model to heterogeneous media, boundary condition (12) is replaced by an equivalent seepage potential condition. The definition of the seepage potential is

$$E = \int_0^{H(x)} K(x,z)(\phi(x,z) - z)dz \ . \tag{22}$$

As the flow domain is bounded by constant heads, there is no recharge and the hydraulic conductivity is constant. The seepage potential, which satisfies $d^2/x^2 = 0$, varies linearly with x as:

$$E = \frac{K}{2}h_0^2 - \frac{K}{2}\frac{x}{L}(h_0^2 - h_w^2) \ . \tag{23}$$

Constructing Nonlinear Equations and the Iteration Method

The nonlinear equations are obtained from the seepage potential and potential function conditions of the phreatic surface. For n positions (i.e., x values), there are 2n unknowns (namely, H(x) and B_m). As the 2n equations obtained from Eqs. (13) and (23) are nonlinear, an iteration scheme is needed. Initial estimates of H(x), based on the Forchheimer solution, and B_m are made at each of the n locations. Then the nonlinear equations are solved by a numerical software "NAG" on the SUN work station. Before solving the equations the seepage face height is assumed. At the end of a calculation the seepage face height is computed by obtaining from Eq. (18) a relation for the stream function (using the Cauchy-Riemann conditions), setting the stream function equal to the flow rate at $z = h_s$ and $x = L$, and solving for h_s. If the computed height differs from the assumed height more than a specified amount, the solution is again computer starting with the computed seepage face height. The flow chart in Figure 8 shows the iteration scheme.

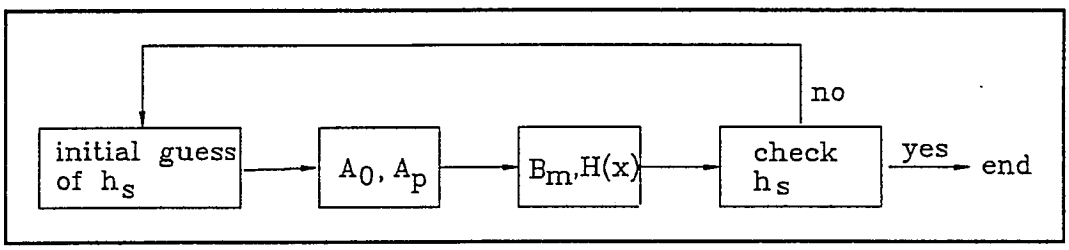

Figure 8. Flow chart of iteration scheme.

RESULTS AND DISCUSSION

Figures 9 and 10 show results of the general method along with values obtained by Murray's method (1970). The comparisons are in dimensionless form for two cases.

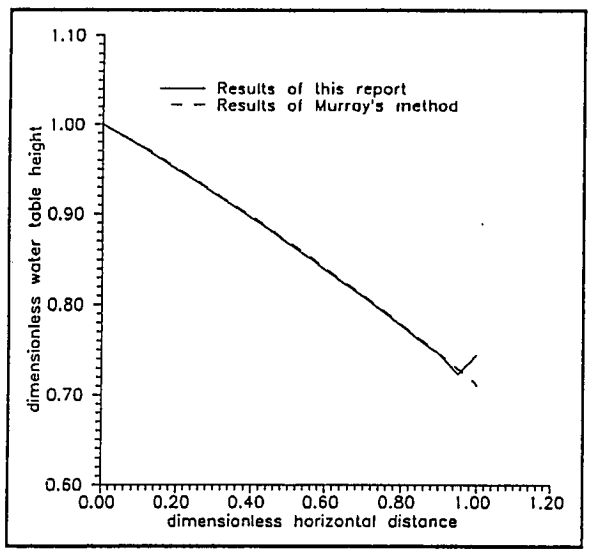

Figure 9. Comparison of phreatic surface water table from the method in this report and Murray's method when $h_w/h_0 = 0.71$.

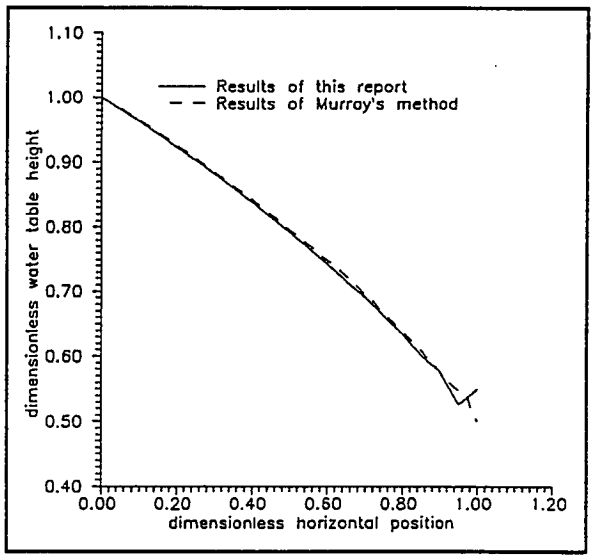

Figure 10. Comparison of phreatic surface water table from the method in this report and Murray's method when $h_w/h_0 = 0.50$.

The results in Figures 9 and 10 show a good match with Murray's method except for the seepage face height. Alternative schemes to express the boundary condition at the point of exit ($z = h_s$, $x = L$), used in computing h_s, are being investigated. Furthermore, as Murray's results are based on the streamline equivalent to Eq. (12), the agreement in Figures 9 and 10 shows that the use of the seepage potential, E, on the water table is equivalent to Eq. (12).

Groundwater mounding will be introduced by supplying a local recharge to the unfoncinfed aquifer. The boundary condition on the phreatic surface, Eq. (12), will be changed to:

$$\left(\frac{K+N}{K}\right)\frac{\partial\phi}{\partial z} - \frac{N}{K} - \left(\frac{\partial\phi}{\partial x}\right)^2 - \left(\frac{\partial\phi}{\partial x}\right)^2 = 0 \qquad (24)$$

where $N > 0, = 0$ under, outside recharge site, respectively, or its equivalent in terms of the seepage potential, E(x).

CONCLUSIONS

A general analytic/numeric method to solve Laplace's equation subject to seepage potential and potential function conditions on the water table has been developed for analyzing mounding in heterogeneous aquifers. For a simple case in a homogeneous aquifer, computed water table heights match well with Murray's results except for the seepage face height. Alternative forms of the exit condition are being investigated to resolve this error. Groundwater mounding will be introduced by supplying a local recharge to the unconfined aquifer and applying the appropriate water table condition. The water table shape and height and the flow pattern are affected by heterogeneity as shown in previous studies (Voorhees, 1989). Simple forms of heterogeneity (e.g., uniform layers of different hydraulic conductivity) will be studied.

REFERENCES

Ahlstrom, S., H. Foote, R. Arnett, C. Cole, and R. Serne. 1977. Multicomponent mass transport model: Theory and numerical implementation. Rep. BNWL 2127, Battelle Pacific Northwest Laboratories, Richland, WA.

Brock, R. R. 1976. Dupuit-Forchheimer and potential theories for recahrge form basins. Water Resources Research 12(5):909-912.

Dagan, G. 1989. Flow and transport in porous formation. Springer-Verlag, Hamburg, Germany.

Girinskii, N. K. 1946. Complex potential of flow with free surface in a stratum of relatively small thickness and k = f(z). (In Russian.) Dokl. Akad. Nauk SSSR 51(5):337-338.

Hantush, M. S. 1967. Growth and decay of groundwater-mounds in response to uniform percolation. Water Resources Research 3(1):227-234.

Kirkham, D. and W. L. Powers. 1964. An exact theory of seepage of steady rainfall into tile and ditch drained land of finite depth. Eight Internal Congress of Soil Science, Bucharest, Romania. pp. 39-44.

Murray, W. A. 1970. Seepage face effects in unsteady groundwater flow. Ph.D. Thesis, Civil and Environmental Engineering, University of Wisconsin-Madison.

Paschke, N. and J. A. Hoopes. 1984. Buoyant contaminant plume in groundwater. Water Resour. Res. 20(9):1183-1192.

Strack, O. D. 1984. Three-dimensional streamlines in Dupuit-Forchheimer models. Water Resources Research 20(7):812-822.

Strack, O. D. L. 1989. Groundwater mechanics. Prentice Hall Englewood Cliffs, NJ.

Tompson, A. F. B. and L. W. Gelhar. 1990. Numerical simulation of solute transport in three-dimensional, randomly, heterogeneous porous media. Water Resour. Res. 26(10):2541-2561.

Tompson, A. F. B., E. G. Vomvoris, and L. W. Gelhar. 1987. Numerical simulation of solute transport in randomly heterogeneous porous media: Motivation, model development, and application. Rep. UCID-21281, Lawrence Livermore National Laboratory, Livermore, CA.

Voorhees, J. 1989. Sand tank mounding experiment results. Civil and Environmental Eingeering independent study report, University of Wisconsin-Madison.

Youngs, E. G. 1965. Horizontal seepage through unconfined aquifers with hydraulic conductivity varying with depth. J. Hydrol. 3:282-296.